Effects of both Shortening and Lengthening the Active Site Nucleophile of *Bacillus circulans* Xylanase on Catalytic Activity†

Sherry L. Lawson,‡ Warren W. Wakarchuk,§ and Stephen G. Withers*,‡

Protein Engineering Network of Centres of Excellence and the Department of Chemistry, University of British Columbia, Vancouver, British Columbia, Canada V6T 1Z1, and the Institute for Biological Sciences, National Research Council of Canada, Ottawa, Ontario, Canada K1A 0R6

Received March 11, 1996; Revised Manuscript Received May 28, 1996⊗

ABSTRACT: The relative positioning of the two carboxyl groups at the active site of glycosidases is crucial to their function and the mechanism followed. The distance between these two groups in *Bacillus circulans* xylanase has been modified by mutagenesis of the catalytic nucleophile Glu78. An increase in the separation (Glu78Asp) results in a large (1600−5000-fold) reduction in the rate of the glycosylation step, but little change in the extent of bond cleavage or proton donation at the transition state. A decrease in the separation was achieved by selective carboxymethylation of the Glu78Cys mutant. This modified mutant was only 16−100-fold less active than wild-type enzyme, and its transition state structure was similarly unchanged. Complete removal of the carboxyl group (Glu78Cys) resulted in a mutant with no measurable catalytic activity. Furthermore, it did not even undergo the first step, glycosylation of the active site thiol. These results confirm the importance of precise positioning of the nucleophile at the active site of these enzymes.

Glycosidases catalyze the hydrolysis of glycosidic bonds by two distinct mechanisms. Retaining glycosidases, which catalyze hydrolysis with net retention of anomeric configuration, employ a double-displacement mechanism involving a covalent glycosyl−enzyme intermediate as illustrated in Scheme 1. By contrast, inverting glycosidases use a direct-displacement reaction to achieve overall inversion of anomeric configuration (Koshland, 1953; Sinnott, 1990). While the two mechanisms are distinct, they possess several important similarities since both proceed via oxocarbenium ion-like transition states and, in both cases, a pair of carboxylic acids function as the catalytic residues. In retaining glycosidases one carboxylic acid functions as an acid/base catalyst and the other as a nucleophile, the average distance between the two essential carboxylic acids being ∼5.5 Å. In inverting enzymes one functions as a general acid and the other as a general base, and the distance between them is greater (∼10 Å), accommodating a water molecule (Wang et al., 1994; White et al., 1994; McCarter & Withers, 1994; Davies & Henrissat, 1995).

Since this separation appears to be a primary determinant of the mechanism followed, it is of interest to explore the mechanistic consequences of altering this critical distance between the two essential carboxylic acids. A good model enzyme system for examining this question is the endo-β-1,4-xylanase from *Bacillus circulans*. A member of the family G (Gilkes et al., 1991; Oku et al., 1993) or family 11 xylanases (Henrissat & Barrioch, 1993), *B. circulans* xylanase is a relatively small retaining glycosidase (20 kDa),

Scheme 1: Proposed Mechanism for a Retaining Glycosidase

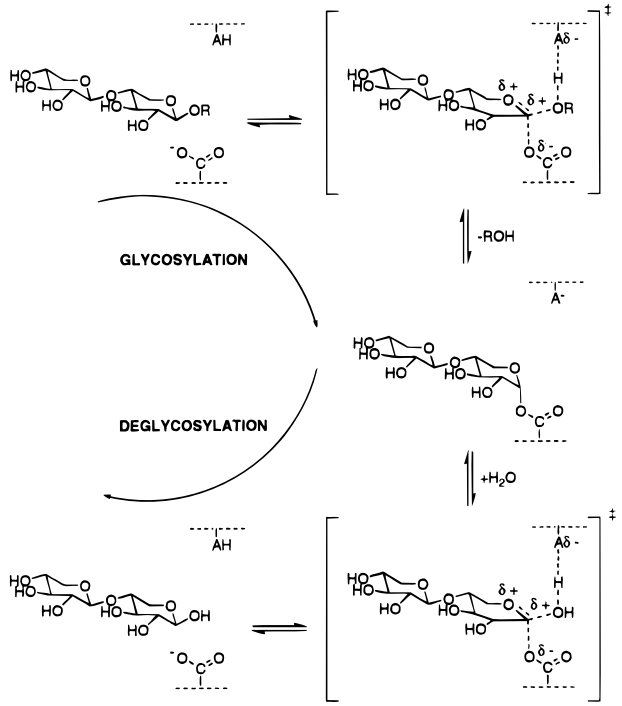

completely free of cysteine residues, for which an X-ray crystal structure is available (Campbell et al., 1993; Wakarchuk et al., 1994; Gebler et al., 1992). Two carboxylic acids, Glu78 and Glu172, are located at the active site, and mutagenesis studies have suggested that these are mechanistically important (Wakarchuk et al., 1994). Identification of Glu78 as the active site nucleophile was achieved by trapping of the covalent glycosyl−enzyme intermediate using a mechanism-based inactivator (Miao et al., 1994). Glu172, therefore, must function as the acid/base catalyst. The key

† This work was supported by funds from the Protein Engineering Network of Centres of Excellence of Canada and the Natural Sciences and Engineering Research Council of Canada.

* To whom correspondence should be addressed.

‡ Department of Chemistry.

§ Institute for Biological Sciences, National Research Council of Canada.

⊗ Abstract published in *Advance ACS Abstracts,* July 15, 1996.

S0006-2960(96)00586-7 CCC: $12.00

catalytic residues of two other family G xylanases, *Schizophyllum commune* and *Bacillus pumilis*, have also been shown to be carboxylic acids (Bray & Clarke, 1990; Katsube et al., 1990; Ko et al., 1992).

One strategy for modifying the distance (~5.5 Å) between Glu78 and Glu172 is to selectively replace each one of the glutamic acids with a shortened or lengthened analogue. The active site nucleophile, glutamic acid 78, was the chosen target for modification. To increase the distance (>5.5 Å) between the two catalytic residues, Glu78 was replaced with aspartic acid, and the mutant was found to have only 0.04% wild-type activity using xylan as the substrate, but no further kinetic studies were performed (Wakarchuk et al., 1994). Similar studies have been conducted with other retaining glycosidases in which the identified active site nucleophile, a glutamic acid, has been replaced with an aspartic acid (Withers et al., 1992; Yuan et al., 1994). In all such studies, shortening the nucleophile's side chain resulted in a very large reduction in activity.

To decrease the distance (<5.5 Å) between the two essential carboxylic acids, Glu78 needs to be replaced with a lengthened carboxylic acid analogue. Since no suitable natural amino acid is available, we first generated a Glu78Cys[1] mutant by site-directed mutagenesis followed by selective reaction with iodoacetate to yield carboxymethylated Cys78, a glutamic acid analogue in which the side chain is lengthened by approximately 1.6 Å. As previously mentioned, wild-type *B. circulans* xylanase contains no cysteines, which eliminates the problem of multiple cysteine labeling. Several other investigators have used this combined approach of genetic engineering with chemical modification to introduce unnatural amino acids into the active sites of other enzymes (Amano et al., 1994; Dhalla et al., 1994; Gloss & Kirsch, 1995; Lukac & Collier, 1988; Matsushima et al., 1994; Planas & Kirsch, 1991; Smith & Hartman, 1988).

This study describes the preparation and characterization of the carboxymethylated Glu78Cys mutant (denoted IAA-Glu78Cys) followed by a detailed kinetic evaluation of this enzyme, native xylanase, and the Glu78Asp mutant.

EXPERIMENTAL PROCEDURES

General. The compounds 2,5-dinitrophenyl β-xylobioside (2,5-DNPX_2), 3,4-dinitrophenyl β-xylobioside (3,4-DNPX_2), *o*-nitrophenyl β-xylobioside (ONPX_2), *p*-nitrophenyl β-xylobioside (PNPX_2), phenyl β-xylobioside (PhX_2), and 2,4-dinitrophenyl 2-deoxy-2-fluoro-β-xylobioside (2F-DNPX_2) were synthesized according to published procedures by Dr. Lothar Ziser (Ziser et al., 1995; Ziser & Withers, 1994). Deuterium oxide (minimum isotopic purity 99.96%) was purchased from the Aldrich Chemical Co., Inc. All other chemicals and buffer materials were obtained from the Sigma Chemical Co. unless otherwise stated.

All spectrophotometric experiments, with the exception of the thiol titrations, were done with 1 cm path length micro black quartz cuvettes using a Unicam 8700 UV/vis spectrophotometer equipped with a circulating water bath. Thiol titrations were performed with plastic cuvettes using a thermostated double-beam UV/vis spectrophotometer (Pye Unicam PU 8800). The circular dichroism (CD) spectra of xylanase (using a protein concentration of 0.2 mg/mL) were obtained with a JASCO J-710 spectropolarimeter. All CD spectra were acquired from 205 to 255 nm and corrected for the buffer background. ^{1}H NMR spectroscopy was performed on a Bruker WH-400 spectrometer, using the HOD signal as an internal standard. All electrospray mass spectrometry (ESMS) experiments were done using an HPLC-ESMS setup consisting of a microbore HPLC (Michrom UMA) connected on-line to a Sciex API III MS as described by Hess et al. (1993). Protein samples (10−20 μg) were injected onto a microbore PLRP column (1 × 50 mm), while a Reliasil C18 column (1 × 150 mm) was used for the proteolytic digests. Following elution with a water−acetonitrile solvent system and UV detection, 15% of the eluant was introduced directly into the MS by an ion spray ion source and analyzed.

Molecular Biology, Enzyme Production, and Purification. The following standard laboratory strains of *Escherichia coli* were used for the propagation of recombinant plasmids and the production of recombinant gene products. MV1190: Δ (*lac-proAB*), *thi*, *supE*44, deletion (*sr*1-*recA*)306::Tn10 (tet^r) [F′: *traD*36, *proAB*, *lacI*^{q} ΔM15]; RZ1032: HfrKL16 PO/45 [*lysA* (61−62)], *dut*1, *ung*1, *thi*1, *relA*1, *Zbd*-279::Tn10, *supE*44; BHM 71−18: Δ (*lac-proAB*), *thi*, *supE*44, [*mutS*::Tn10 (tet^r)], [F′: *proAB*, *lacI*^{q} ΔM15]; HB101: *hsdS*20 (r-m-), *leu*, *supE*44, *ara*14, *galK*2, *lacY*1, *proA*2, *rpsL*20 (Str^r), *xy1*-5, *mt1*-5, *recA*13, *mcrB*.

The mutagenesis, detection of xylanase mutants, and the production and purification of mutant proteins and wild-type xylanase was performed as previously described (Sung et al., 1993; Wakarchuk et al., 1994). The oligonucleotides for mutagenesis of *B. circulans* xylanase were for Glu78Cys, 5′ C AAC GTA ATA **GCA** AAT CAG TGG C [this primer uses the synthetic gene [see Sung et al. (1993)] as a template], and for Glu78Asp, 5′ T CTC ATA **GAC** TAT TAT GTA [this primer was used with the natural gene in pUC118 and then the mutant was subcloned into the expression vector previously described (Wakarchuk et al., 1994)].

Basic recombinant DNA methods like plasmid DNA isolation, restriction enzyme digestions, the purification of DNA fragments for cloning, ligations, transformations, and DNA sequencing were performed as recommended by the enzyme supplier or the manufacturer of the kit used for the particular procedure. Restriction and DNA modification enzymes were purchased from New England Biolabs Ltd., Mississauga, ON. Prep-A-Gene DNA purification matrix was purchased from Bio-Rad laboratories, Mississauga, ON. Sequenase, DNA sequencing kit was purchased from US Biochemicals, Cleveland, OH. Oligonucleotide 3′ end labeling with digoxigenin-ddUTP and the subsequent chemiluminescent detection were performed with a kit and some

[1] Abbreviations: BSA, bovine serum albumin; CAPSO, 3-(cyclohexylamino)-2-hydroxy-1-propanesulfonic acid; CD, circular dichroism; DNP, dinitrophenolate; 2,5-DNPX_2, 2,5-dinitrophenyl β-xylobioside; 3,4-DNPX_2, 3,4-dinitrophenyl β-xylobioside; EDTA, ethylenediaminetetraacetic acid; ESMS, electrospray mass spectrometry; 2F-DNPX_2, 2,4-dinitrophenyl 2-deoxy-2-fluoro-β-xylobioside; Glu78Asp, *B. circulans* xylanase in which Glu78 has been replaced with an Asp; Glu78Cys, *B. circulans* xylanase in which Glu78 has been replaced with a Cys; HEPES, *N*-(2-hydroxyethyl)piperazine-*N*′−2-ethanesulfonic acid; HPLC, high-performance liquid chromatography; IAA, iodoacetate; IAA-Glu78Cys, Glu78Cys carboxymethylated at Cys78; LC, liquid chromatography; MES, 2-(*N*-morpholino)ethanesulfonic acid; MMTS, methyl methanethiolsulfonate; MS, mass spectrometry; MWt, molecular weight; NMR, nuclear magnetic resonance; ONPX_2, *o*-nitrophenyl β-xylobioside; PhX_2, phenyl β-xylobioside; PNPX_2, *p*-nitrophenyl β-xylobioside; TIC, total ion chromatogram.

additional reagents from Boehringer Mannheim Canada, Laval, PQ.

Iodoacetate Labeling of the Glu78Cys Mutant under Nondenaturing Conditions. Enzyme (2 mg/mL; 0.1 mM) was incubated, in the dark, with 120 mM iodoacetate (IAA), 150 mM CAPSO, and 1 mM EDTA, pH 10, at 36 °C. A pH of approximately 10 was maintained through periodic additions of 1 M NaOH. Reactivation of the enzyme was followed by assaying aliquots of the reaction mixture with 1.2 mM 2,5-DNPX$_2$. Upon reaching maximal reactivation, excess reagent was removed by applying the reaction mixture to a Sephadex G-25 column. After the column was eluted with 50 mM MES (pH 6.5), the appropriate fractions were pooled and concentrated using 10 kDa nominal cut-off centrifugal concentrators (Amicon Corp., Danvers, MA). The protein concentration was determined from the molar extinction coefficient for xylanase: $\epsilon = 81\,790$ L mol^{-1}, $A_{280}^{0.1\%} = 4.08$ (Wakarchuk et al., 1994).

Iodoacetate Labeling of the Glu78Cys Mutant under Denaturing Conditions. Enzyme (1 mg/mL; 0.05 mM) in 7.1 M urea, 11% glycerol, 400 mM glycylglycine, 40 mM HEPES, and 1 mM EDTA (pH 7.5) was incubated for 20 min at 60 °C. The reaction mixture was cooled to 40 °C, and IAA was added to give a final reagent concentration of 0.5 mM. After incubating in the dark for 19 h, the reaction mixture was diluted 20 times with the above 7.1 M urea solution and dialyzed against 20 mM HEPES, 10% glycerol buffer (pH 7.0, room temperature, 48 h). The dialyzed sample was filtered through a 0.2 μm filter and concentrated using a 10 kDa nominal cut-off centrifugal concentrator, and its protein concentration was determined.

Methyl Methanethiolsulfonate (MMTS) Labeling of the Glu78Cys Mutant. Enzyme (2 mg/mL; 0.1 mM) in 16 mM glycylglycine, 1 mM EDTA buffer (pH 8.0) was reacted with 10 mM MMTS for 25 h at 4 °C. Excess reagent was removed by diluting the reaction mixture 20-fold with 20 mM MES, 50 mM NaCl buffer (pH 6.0) and then concentrating the sample down to its original volume using a 10 kDa nominal cut-off centrifugal concentrator (repeated three times).

Thiol Titrations. The number of free thiol groups was determined using the method of Ellman (1959). To a solution of 0.2 mM 5,5′-dithiobis(2-nitrobenzoic acid), 6 M guanidine hydrochloride, 20 mM HEPES, and 1 mM EDTA (pH 7.4) warmed to 25 °C was added enzyme (2.5−5 μM). The absorbance at 412 nm, due to the released 2-nitro-5-thiobenzoate, was monitored over a 30 min period. The concentration of free thiol groups was calculated from the net ΔA_{412}, corrected for a buffer blank, using the extinction coefficient $\epsilon = 13\,591$ M^{-1} cm^{-1} (determined from a cysteine standard curve generated under the same conditions). Division of this obtained value by the protein concentration yielded the number of free thiol groups.

Active Site Titration of the IAA-Glu78Cys Mutant Using 2F-DNPX$_2$. To a solution of 1.6 mM 2F-DNPX$_2$, 20 mM MES, and 50 mM NaCl (pH 6.0) warmed to 25 °C was added enzyme (final concentration of 1 mg/mL; 0.05 mM). The 2,4-dinitrophenolate released, due to inactivation of the active enzyme, was monitored at 400 nm. The increase in the A_{400} observed was corrected for the absorbance due to the spontaneous hydrolysis of the inactivator. From the net ΔA_{400} the concentration of 2,4-dinitrophenolate released, and thereby the concentration of active enzyme, was determined ($\Delta\epsilon = 10.80$ mM^{-1} cm^{-1}). The complete inactivation of IAA-Glu78Cys was confirmed by assaying an aliquot of the reaction mixture with 1.2 mM 2,5-DNPX$_2$.

Steady-State Kinetic Studies. The rates of enzymatic hydrolysis for all the substrates, with the exception of PhX$_2$, were determined using a continuous assay. An appropriate concentration of substrate in 20 mM MES, 50 mM NaCl buffer, pH 6.0, containing 0.1% BSA was warmed to 40 °C. Reaction was initiated by the addition of enzyme. Substrate hydrolysis was monitored by measuring the rate of phenolate release at the appropriate wavelength: 2,5-DNPX$_2$, 440 nm, $\Delta\epsilon = 3.57$ mM^{-1} cm^{-1}; 3,4-DNPX$_2$, 400 nm, $\Delta\epsilon = 11.71$ mM^{-1} cm^{-1}; ONPX$_2$, 400 nm, $\Delta\epsilon = 1.07$ mM^{-1} cm^{-1}; PNPX$_2$, 400 nm, $\Delta\epsilon = 1.66$ mM^{-1} cm^{-1}.

Xylanase-catalyzed hydrolysis rates for the substrate PhX$_2$ were determined using a stopped assay. Different concentrations of PhX$_2$ in 0.1% BSA, 20 mM MES, 50 mM NaCl buffer (pH 6.0, 190 μL) were warmed to 40 °C, and the reaction was initiated by the addition of a 10 μL aliquot of enzyme. After an appropriate time, 0.6 mL of 0.2 M Na_3PO_4/H_2O (pH 12.15) was added to stop the reaction. The absorbance of the released phenolate at 288 nm was determined immediately and corrected for the spontaneous hydrolysis of PhX$_2$ and the background absorbance of the enzyme ($\Delta\epsilon = 2.17$ mM^{-1} cm^{-1} for phenol at pH 12.15).

Rates were determined at 4−9 different substrate concentrations ranging from 0.02 to 4 times the estimated K_m value, where possible. For some substrates, as noted in Table 1, the high K_m value and the relative insolubility of the substrate precluded study at substrate concentrations above the K_m value. From the experimental rate versus substrate concentration data, values of K_m and k_{cat} were calculated directly using the program GraFit (Leatherbarrow, 1990), while the k_{cat}/K_m values were determined from the slope of the Lineweaver−Burk plot.

To examine whether the observed activity for the Glu78Cys mutant was real or due to a contaminant, the following experiment was performed. The enzyme (9.7 mg/mL; 0.47 mM) was incubated at 40 °C with 0.043 mM 2F-DNPX$_2$, 20 mM MES, and 50 mM NaCl (pH 6.0). At time intervals, residual activity was determined by assaying an aliquot of the inactivation mixture with 1 mM 2,5-DNPX$_2$.

2F-DNPX$_2$ Inactivation Kinetics. The IAA-Glu78Cys mutant (0.26 mg/mL; 0.013 mM) was incubated at 40 °C with different concentrations of 2F-DNPX$_2$ (0, 0.46, 0.68, 1.08, and 1.91 mM) in 0.1% BSA, 20 mM MES, and 50 mM NaCl (pH 6.0). At time intervals, residual enzyme activity was determined by assaying a 5 μL aliquot of the inactivation mixture with 2,5-DNPX$_2$ (1.16 mM). Due to the low solubility of 2F-DNPX$_2$, only inactivator concentrations below the estimated K_i value could be examined. Thus an accurate k_i/K_i value was calculated from the slope of the reciprocal plot ($1/k_{obs}$ vs 1/[I]), and approximate estimates of k_i and K_i were made.

Reactivation of 2F-DNPX$_2$ Inactivated Xylanase. The IAA-Glu78Cys mutant (0.4 mg/mL; 0.02 mM) was incubated with 1.9 mM 2F-DNPX$_2$, 20 mM MES, and 50 mM NaCl (pH 6.0) at 40 °C for 2 h, at which time less than 5% activity remained. Excess inactivator was removed by concentrating the sample using a 10 kDa nominal cut-off centrifugal concentrator, diluting 10-fold with the above buffer, and reconcentrating (repeated twice). Inactivated enzyme (0.10

Table 1: Kinetic Parameters for Aryl β-Xylobiosides with Native Xylanase and Mutants

substrate	kinetic parameter	native	IAA-Glu78Cys	Glu78Asp
2,5-DNPX$_2$ (pK_a = 5.15)[a]	k_{cat} (s^{-1})	76 ± 1.5[c]	21 ± 1.9[d]	0.026 ± 0.0005
	K_m (mM)	2.2 ± 0.1[c]	10 ± 1.2[d]	2.4 ± 0.1
	k_{cat}/K_m (s^{-1} mM^{-1})[b]	35 ± 1.1[c]	2.2 ± 0.03[d]	0.011 ± 0.0002
3,4-DNPX$_2$ (pK_a = 5.36)[a]	k_{cat} (s^{-1})	8.3 ± 0.4[c]	1.6 ± 0.2[d]	0.005 ± 0.0002
	K_m (mM)	3.4 ± 0.3[c]	31 ± 6.1[d]	9.2 ± 0.8
	k_{cat}/K_m (s^{-1} mM^{-1})[b]	2.7 ± 0.1[c]	0.042 ± 0.001[d]	0.0006 ± 2 × 10^{-5}
ONPX$_2$ (pK_a = 7.22)[a]	k_{cat} (s^{-1})	9.6 ± 0.1	1.3 ± 0.04	0.005 ± 0.0002
	K_m (mM)	14.2 ± 0.5	54 ± 3.5	14.4 ± 1.6
	k_{cat}/K_m (s^{-1} mM^{-1})[b]	0.66 ± 0.01	0.021 ± 0.0003	0.0004 ± 9 × 10^{-6}
PNPX$_2$ (pK_a = 7.18)[a]	k_{cat} (s^{-1})	24 ± 2.1	>0.3[d,e]	0.008 ± 0.0001[d]
	K_m (mM)	49 ± 6.4	>25[d,e]	80 ± 1.5[d]
	k_{cat}/K_m (s^{-1} mM^{-1})[b]	0.43 ± 0.01	0.013 ± 0.0002[d,e]	9.0×10^{-5} ± 1 × 10^{-6} [d]
PhX$_2$ (pK_a = 9.99)[a]	k_{cat} (s^{-1})	0.051 ± 0.004	0.002 ± 8 × 10^{-5} [d]	—[f]
	K_m (mM)	8.7 ± 1.3	31 ± 2.2[d]	—[f]
	k_{cat}/K_m (s^{-1} mM^{-1})[b]	0.005 ± 0.0003	5.0 × 10^{-5} ± 9 × 10^{-7} [d]	—[f]

[a] The pK_a value given is for the aglycon. [b] All the k_{cat}/K_m values were determined from the slope of the Lineweaver−Burk plot. [c] Data taken from Ziser et al. (1995). [d] The highest substrate concentration tested was $<K_m$. [e] No saturation kinetics were observed for the substrate range examined (2−22 mM). [f] Enzyme catalyzed hydrolysis was not detected.

mg/mL) in 0.1% BSA, 20 mM MES, and 50 mM NaCl (pH 6.0) was then incubated at 40 °C with either buffer or 155 mM xylobiose until full reactivation was observed. At time intervals, 5 μL aliquots of the reactivation mixture were removed and assayed for activity. The activity versus time data was corrected for enzyme inactivation due to denaturation (from a control experiment). The first-order rate constants for reactivation ($k_{re,obs}$) were obtained from the slope of plots of ln(full rate minus observed rate) versus time.

The pH Dependence of k_{cat}/K_m. Values of k_{cat}/K_m for the hydrolysis of ONPX$_2$ at each pH were determined from progress curves at low substrate concentrations as follows. A solution of ONPX$_2$ (0.5 mM, 0.01K_m and 0.3 mM, 0.02K_m for the IAA-Glu78Cys mutant and native xylanase, respectively), 0.1% BSA, and the appropriate buffer was warmed to 25 °C. A 10 μL aliquot of enzyme (or buffer) was added and the release of *o*-nitrophenolate monitored at 400 nm until greater than 75% substrate depletion was observed. The pH of the reaction mixture was then determined and an aliquot assayed for activity, at pH 6.0, to check enzyme stability. The progress curves were analyzed using a first-order rate equation. The pseudo-first-order rate constants, obtained from this analysis, were then divided by the enzyme concentration to give the k_{cat}/K_m values. The buffers used were as follows: 20 mM succinic acid, 50 mM NaCl (pH 3−5); 20 mM MES, 50 mM NaCl (pH 5−7); 20 mM HEPES, 50 mM NaCl (pH 7−8).

ESMS Analysis of Digested IAA-Glu78Cys. The IAA-Glu78Cys mutant and 2F-DNPX$_2$ inactivated enzyme were digested as follows. Both enzymes were first heat-denatured by boiling for 2 min. The denatured enzymes (20 μL, 4.6 mg/mL) were then incubated with 70 μL of pepsin (0.14 mg/mL) in 50 mM sodium phosphate buffer (pH 2) at room temperature for 12 h. ESMS analysis of the proteolytic digests confirmed that both samples were completely digested. A neutral loss LC-MS/MS experiment was performed as previously described (Miao et al., 1994). In neutral loss LC-MS/MS mode, mass spectra were obtained where Q1 and Q3 are offset by 133.5 Da and only those ions that lose 133.5 Da in the *m*/*z* range of 300−1700 (0.5 Da step) are detected. A subsequent daughter ion MS/MS experiment of the single peptide which underwent neutral loss was carried out by selectively introducing the doubly charged *m*/*z* 842.5 ion through Q1 into the collision cell (Q2) and observing the daughter ions in Q3. The scan range for Q3 was set from 50 to 1700 Da at 1 Da step sizes so that it would capture the entire mass range of the possible daughter ions as well as the parent ion. The collision gas thickness for the daughter ion MS/MS and neutral loss MS/MS experiment was set at approximately 438 (4.38 × 10^{14} molecules/cm^2) and 355 (3.55 × 10^{14} molecules/cm^2), respectively.

Determination of the Stereochemical Course of Hydrolysis. The substrate 2,5-DNPX$_2$ and the buffer, 10 mM sodium phosphate and 50 mM NaCl (pH 6.0), were freeze-dried from D_2O three times. The IAA-Glu78Cys mutant was repeatedly diluted with D_2O buffer and reconcentrated using a 10 kDa nominal cut-off centrifugal concentrator. For both substrate and enzyme, the D_2O used in the final washing had an isotopic purity of 99.96%. To a 5 mm NMR tube was added 0.5 mL of 5.4 mM 2,5-DNPX$_2$, 10 mM sodium phosphate, and 50 mM NaCl (pH 6.0) in D_2O (99.96%). After recording the initial NMR spectrum of substrate and buffer, enzyme (6 μL, 7.5 mg/mL) was added. The stereochemical course of the reaction was monitored, at 25 °C, by collecting spectra at time intervals over a 72 min period.

RESULTS

Preliminary Characterization of the Glu78Cys and Glu78Asp Mutants. The introduction of a unique cysteine in the Glu78Cys mutant was confirmed by both thiol titrations and electrospray mass spectrometry (ESMS). The Cys mutant contained 1.07 (±0.03) free cysteines, as opposed to native xylanase which contained 0.06 (±0.06). The expected molecular mass decrease of 26 Da, due to replacement of a glutamic acid with a cysteine, was observed. For native xylanase and Glu78Cys, the molecular masses were 20 384 (±3) Da and 20 359 (±4) Da, respectively (the theoretical molecular masses are 20 384 and 20 358 Da). The replacement of a glutamic acid with an aspartic acid, in Glu78Asp, was also confirmed by ESMS. The observed molecular mass of Glu78Asp was 20 358 (±4) Da (the

theoretical mass is 20 356 Da).[2] Close similarities between the CD spectra of the Cys and Asp mutants, relative to native xylanase, suggests that the mutations have not significantly altered the enzymes' conformation (data not shown).

Activity of the Glu78Cys Mutant with 2,5-DNPX$_2$. Replacement of Glu78 with a cysteine has a dramatic effect on activity. The apparent k_{cat} and K_m values for the Cys mutant, assayed with 2,5-DNPX$_2$, were 1.1×10^{-5} s^{-1} ($\pm 1.1 \times 10^{-6}$) and <0.7 mM, respectively. Since the mutant exhibited such low activity on 2,5-DNPX$_2$, the most reactive substrate at our disposal, no other substrates were tested.

The extremely low activity of the Glu78Cys mutant raised concerns that the activity might be due to contamination with wild-type enzyme. An experiment using the mechanism-based inactivator 2F-DNPX$_2$ was performed to address this concern. Reaction of the mutant (95 nmol) with 2F-DNPX$_2$ (8.6 nmol) resulted in complete activity loss in 90 min. The observed activity cannot, therefore, be due to the Glu78Cys mutant since all activity was lost upon treatment with only 0.09 equiv of inactivator. This was confirmed by ESMS analysis of the sample after inactivation, with identical molecular masses being observed for treated and untreated mutant (20 358 ± 4 Da). The low activity observed for Glu78Cys is therefore likely due to very low levels of contaminating wild-type or another active mutant. Given the greater than 3-fold K_m difference for Glu78Cys relative to wild type, the wild-type enzyme is the least likely candidate.

Iodoacetate Labeling of the Glu78Cys Mutant under Nondenaturing Conditions. Preliminary work indicated that the Glu78Cys mutant could be reactivated by iodoacetate (IAA) treatment without denaturation. A wide range of conditions of pH (from pH 7 to 11), buffer species, and IAA concentrations (10−2000-fold molar excess) were investigated, the largest observed activity regain occurring when the Cys mutant (0.1 mM) was incubated with 1200 times excess IAA (120 mM) for 27 h (36 °C, pH 10, CAPSO). ESMS analysis of the labeled enzyme showed significant multiple labeling, with at least six different amino acids being modified by IAA. Reaction with methyl methanethiolsulfonate (MMTS), which blocks the cysteine with a thiomethyl group (47 Da), was, however, selective. ESMS analysis of this modified enzyme revealed a single species with a molecular mass 43 (±4) Da greater than untreated Glu78Cys, as expected. Reaction of this MMTS-modified Glu78Cys mutant with IAA, using the conditions described above, resulted in no reactivation, strongly suggesting that the carboxymethylation of Cys78 is responsible for the observed reactivation of the Glu78Cys mutant.

In order to determine what fraction of the IAA-labeled Glu78Cys mutant was active, an active site titration with 2F-DNPX$_2$ was carried out. Incubation of labeled enzyme (0.16 mM) with 2F-DNPX$_2$ (1.6 mM) resulted in time-dependent inactivation and a burst of released 2,4-dinitrophenolate (2,4-DNP) ($\Delta A = 0.109$) was measured at 400 nm. Since 1 mol of 2,4-DNP is released per mol of "active" enzyme, the magnitude of this burst indicates that only approximately 7% of the IAA-labeled enzyme was active.

[2] The Glu78Asp mutant is from *Bacillus subtilis* rather than *Bacillus circulans*. The xylanases from these two species are identical in activity and other properties, only differing in the amino acid residue at position 147 (in *B. circulans* it is a threonine, while in *B. subtilis* it is a serine). The theoretical mass of native xylanase from *B. subtilis* is 20 370 Da.

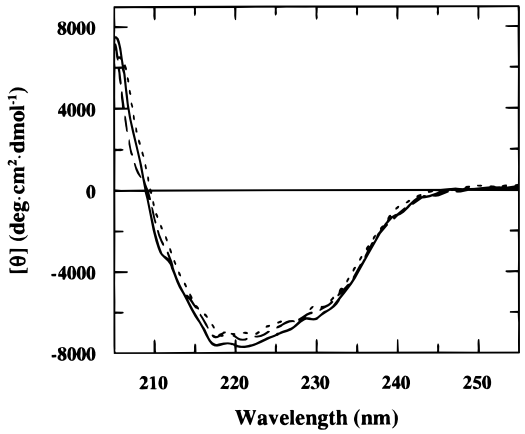

FIGURE 1: CD spectra of refolded IAA-treated Glu78Cys (- - -) and native xylanase (— —). The CD spectrum of untreated native xylanase (—) was run as a control.

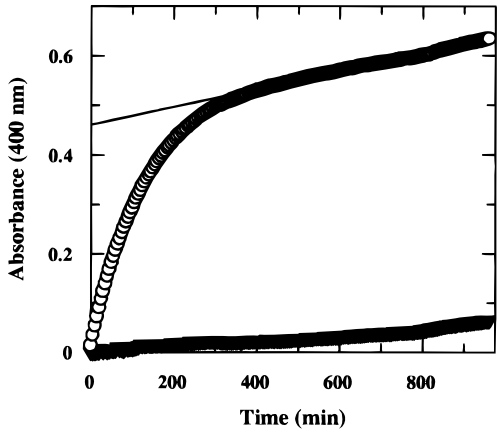

FIGURE 2: Active site titration of IAA-Glu78Cys prepared under denaturing conditions. The time-dependent release of 2,4-dinitrophenolate in the presence of IAA-Glu78Cys (○) and buffer (▼) was monitored at 400 nm.

Iodoacetate Labeling of the Glu78Cys Mutant under Denaturing Conditions. Since IAA labeling of Glu78Cys under nondenaturing conditions was nonselective, producing less than 7% active enzyme, IAA labeling was performed under denaturing conditions, to improve the selectivity, and the labeled enzyme was then refolded. ESMS analysis of the labeled mutant (IAA-Glu78Cys) showed >90% conversion of Glu78Cys to a monolabeled species having a molecular mass of 20 420 (±4) Da (the theoretical molecular mass of IAA-Glu78Cys is 20 416 Da, and the mass of untreated Glu78Cys was 20 362 ± 3 Da). Native xylanase exposed to the same labeling conditions showed no sign of labeling by ESMS, thus suggesting that the amino acid alkylated in the mutant is Cys78. Thiol titrations on the IAA-Glu78Cys mutant and a control sample (exposed to similar conditions, but in the absence of IAA) confirmed the selective alkylation of Cys78, the samples having 0.12 and 0.92 free cysteines, respectively. The CD spectra of the labeled Cys mutant and native xylanase, shown in Figure 1, are virtually superimposable, indicating that correct refolding has occurred.

An active site titration using 2F-DNPX$_2$ was then performed to determine the amount of active IAA-Glu78Cys formed. The results, illustrated in Figure 2, show the release of 2,4-dinitrophenolate as a burst followed by a steady state. From the magnitude of the burst (observed $\Delta A_{400} = 0.48$, expected $\Delta A_{400} = 0.53$), it was estimated that greater than

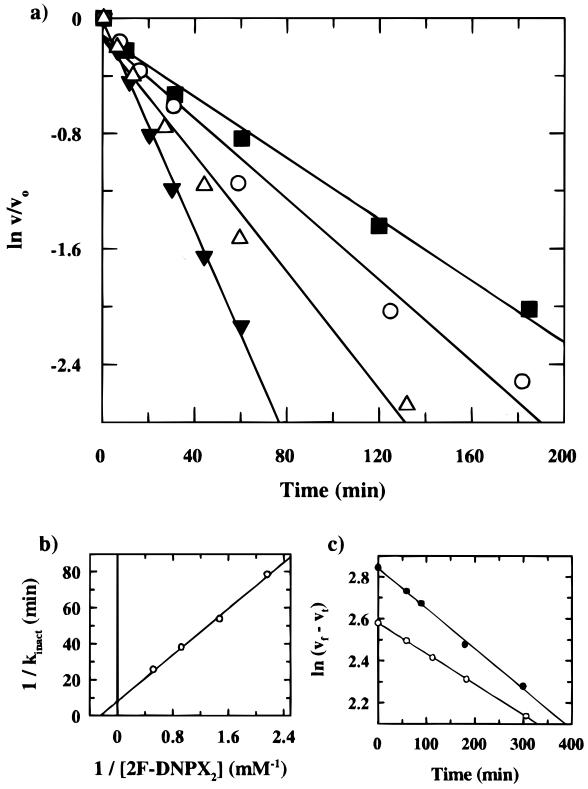

FIGURE 3: Inactivation of IAA-Glu78Cys (prepared under denaturing conditions) by 2F-DNPX$_2$. (a) Semilogarithmic plot of residual activity vs time at the following inactivator concentrations: 0.46 mM (■), 0.68 mM (○), 1.08 mM (△), and 1.91 mM (▼). (b) The double-reciprocal plot of the first-order rate constants obtained from panel a. (c) The reactivation of inactivated IAA-Glu78Cys by 155 mM xylobiose (●) and buffer (○) (v_f is the rate at complete reactivation, and v_t is the observed rate at time t).

Scheme 2

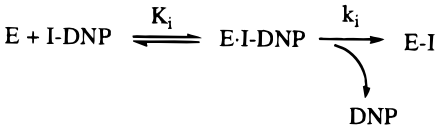

90% of the enzyme was active. The steady-state rate observed is a combination of spontaneous hydrolysis of 2F-DNPX$_2$ and enzyme-catalyzed turnover. Assay of the IAA-Glu78Cys mutant after completion of this burst phase revealed an activity of less than 4% of the control. The molecular masses of the inactivated enzyme and a control were 20 684 (±4) Da and 20 420 (±3) Da, respectively, the molecular mass difference of 264 Da confirming the covalent attachment of the 2-fluoroxylobiosyl label (267 Da). All subsequent experiments were performed on IAA-Glu78Cys prepared under denaturing conditions.

Kinetic Analysis of the 2F-DNPX$_2$ Inactivation. The time-dependent inactivation of IAA-Glu78Cys by 2F-DNPX$_2$, first demonstrated in the active site titration experiment, was examined more closely by determining the inactivation rates at a series of inactivator concentrations. The kinetic scheme shown in Scheme 2 was followed, where E corresponds to free enzyme, I to 2F-xylobiose, and DNP to 2,4-dinitrophenolate. From these results, seen in Figure 3a,b, the values for k_i (0.10 ± 0.007 min^{-1}), K_i (3.2 ± 0.3 mM), and k_i/K_i (0.031 min^{-1} mM^{-1}) were determined. Kinetic parameters for the inactivation of native xylanase by 2F-DNPX$_2$ had previously been determined as $k_i = 2.2 \pm 0.6$ min^{-1}, $K_i = 6.4 \pm 2.1$ mM, and $k_i/K_i = 0.34$ min^{-1} mM^{-1} (Miao et al., 1994). Values of k_i and K_i given are very approximate since the relative insolubility of the inactivator precluded study at 2F-DNPX$_2$ concentrations even approaching its K_i value. However, the k_i/K_i value, determined from the slope of the reciprocal plot in Figure 3b, is accurate.

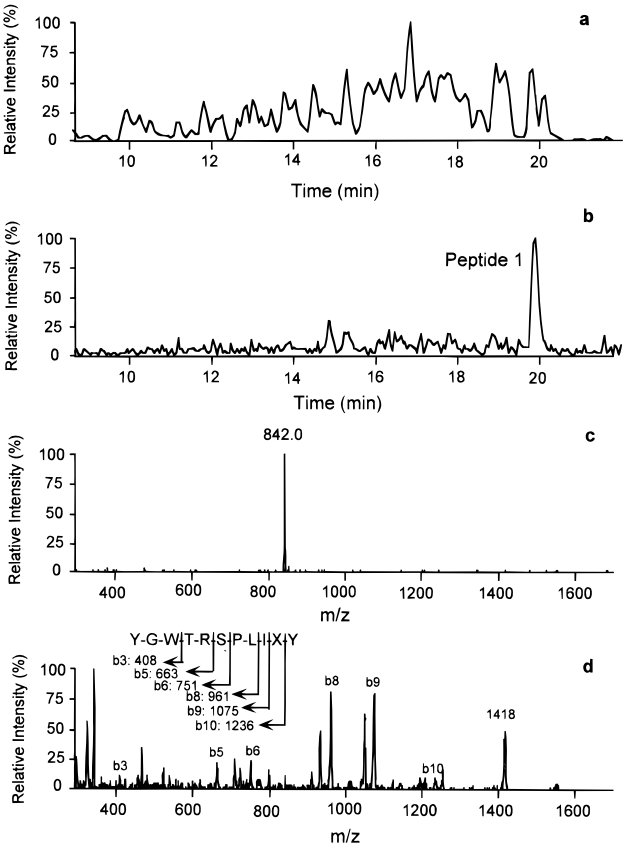

FIGURE 4: ESMS analysis of digested 2F-DNPX$_2$ inactivated IAA-Glu78Cys (prepared under denaturing conditions). (a) TIC in normal MS mode, (b) TIC in neutral loss mode, (c) mass spectrum of peptide 1 in panel b, and (d) MS/MS daughter ion spectrum of the 2-fluoroxylobiosyl labeled peptide (*m*/*z* 842.0 in the doubly charged state).

Reactivation of the Inactivated IAA-Glu78Cys Mutant. Inactivated IAA-Glu78Cys, freed of excess 2F-DNPX$_2$, was incubated with buffer or xylobiose (155 mM) at 40 °C, and aliquots were assayed for activity regain due to regeneration of free enzyme. The data, shown in semilogarithmic form in Figure 3c, yielded the following reactivation rate constants, $k_{re,obs} = 0.00150 \pm 0.00001$ min^{-1} and 0.00190 ± 0.00006 min^{-1}, for buffer and 155 mM xylobiose, respectively. The reactivation of 2F-DNPX$_2$ inactivated native xylanase, incubated with just buffer, also occurred via a first-order process with a $k_{re,obs} = 0.0021$ min^{-1} (Miao et al., 1994).

Identification of the 2-Fluoroxylobiosyl Labeled Active Site Peptide by ESMS. The 2F-DNPX$_2$ inactivated IAA-Glu78Cys mutant and a control (not exposed to 2F-DNPX$_2$) were digested using pepsin. The resulting peptide mixtures were separated by reverse-phase HPLC using the ESMS as a detector (Figure 4a). The peptide bearing the 2-fluoroxylobiosyl label was located in this chromatogram by MS/MS analysis using a neutral loss experiment [refer to Experimental Procedures and Miao et al. (1994) for a complete description]. When the spectrometer was scanned for the mass loss *m*/*z* 133.5, corresponding to the loss of the sugar label from a doubly charged peptide, a single peak was

observed in the TIC (Figure 4b). This unique peak, having a *m*/*z* of 842.0 and a retention time of ~20 min, was not detected in the control digest (data not shown). Since the doubly charged, labeled peptide has a *m*/*z* 842.0, the singly charged, unlabeled peptide must have a molecular mass of 1417 Da [(2 × 842) − 267]. A computer-generated search for all peptides in the IAA-Glu78Cys mutant with a molecular mass of 1417 ± 2 Da yielded 13 possible peptides, three of which contained the expected carboxymethylated Cys78.

Sequence information on the 2-fluoroxylobiosyl labeled peptide was obtained by performing an MS/MS experiment at higher collision energies (as described in Experimental Procedures). The parent ion of *m*/*z* 842.0 was selected in the first quadrupole, subjected to collision-induced fragmentation in a collision cell in the second quadrupole, and the mass of the daughter ions produced detected in the third quadrupole. The family of daughter ions produced is shown in Figure 4d. The daughter ion at *m*/*z* 1418 arises from the loss of the 2-fluoroxylobiosyl label plus a proton from the parent ion (to give the singly charged unlabeled peptide). Further fragmentations observed represent loss of fragments from the C-terminus. The peak at *m*/*z* 1236 (b10) is attributed to the loss of the C-terminal tyrosine (*m*/*z* 181) from the peak at *m*/*z* 1418. The other peaks (b9, b8, b6, b5, and b3) result from the respective losses of XY, IXY, PLIXY, SPLIXY, and TRSPLIXY fragments from the C-terminus. A parallel "a" series of ions is also observed and results from the additional loss of CO (28 Da) from the peaks in the "b" series. This sequence information, combined with the xylanase sequence and the mass of the intact peptide, is sufficient to identify the 2-fluoroxylobiosyl labeled peptide as YGWTRSPLIXY (where X corresponds to a carboxymethylated cysteine).

Determination of the Stereochemical Course of Hydrolysis. The hydrolysis of the substrate 2,5-DNPX_2 by the IAA-Glu78Cys mutant was monitored using ^{1}H NMR spectroscopy. Figure 5a shows the anomeric proton region of 2,5-DNPX_2 in buffer, prior to addition of enzyme. The doublet at δ 5.29 ppm (J = 6.8 Hz) arises from the axial anomeric proton of the substrate, while the singlet at δ 4.48 ppm (marked x) is due to an impurity in the D_2O. Eight minutes after the addition of the labeled mutant (Figure 5b), the doublet at δ 5.29 ppm has almost disappeared and a new doublet (δ 4.47 ppm, J = 7.8 Hz), due to the anomeric proton of β-xylobiose, has appeared. Figure 5c, taken 20 min after enzyme addition, shows complete substrate hydrolysis and the emergence of a new doublet at δ 5.06 ppm (J = 3.6 Hz) which is increased further in intensity at 72 min (Figure 5d). This new doublet arises from the anomeric proton of α-xylobiose which is formed by mutarotation of the initially formed β-xylobiose.

Kinetic Evaluation of Native Xylanase, Glu78Asp, and the IAA-Glu78Cys Mutant. The kinetic parameters k_{cat}, K_m, and k_{cat}/K_m were determined for a series of aryl β-xylobioside substrates and are summarized in Table 1. Values of k_{cat} and k_{cat}/K_m for IAA-Glu78Cys are based upon the assumption of 100% labeling, consistent with the active site titration performed (90 ± 10% labeling). For some substrates, as indicated in Table 1, the highest substrate concentration tested was below the listed K_m value. For these substrates, the k_{cat} and K_m values given in Table 1 are less accurate than the errors would suggest, but the k_{cat}/K_m values, determined from the slope of the Lineweaver−Burk plot, are accurate. For

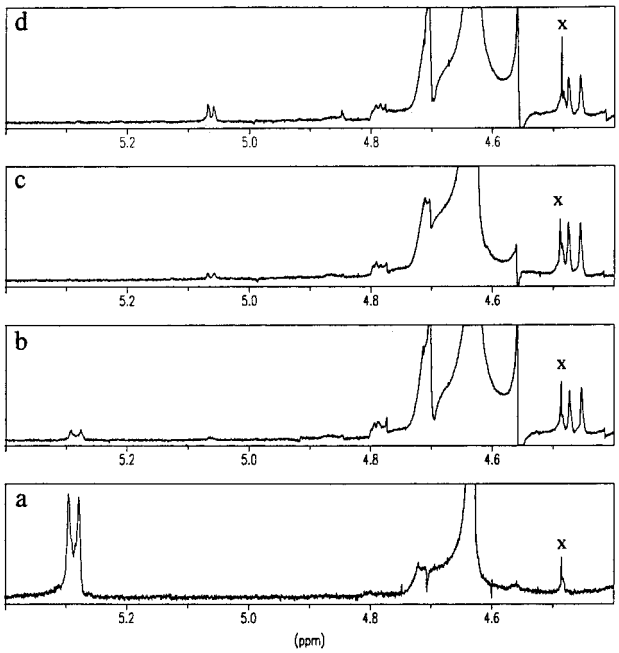

FIGURE 5: Determination of the stereochemical course of hydrolysis of 2,5-DNPX_2 by IAA-Glu78Cys (prepared under denaturing conditions). ^{1}H NMR spectra are for the anomeric proton region of the substrate before addition of enzyme (a) and 8, 20, and 72 min after enzyme addition (b, c, and d, respectively).

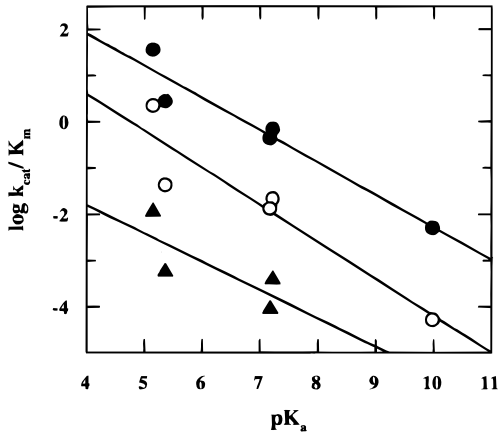

FIGURE 6: Brønsted plot (log k_{cat}/K_m vs aglycon pK_a) for native xylanase (●), the Glu78Asp mutant (▲), and the IAA-Glu78Cys mutant (○) prepared under denaturing conditions.

the three enzyme species the Brønsted relationships between log k_{cat}/K_m for each substrate and the pK_a of the aglycon are presented in Figure 6. For native xylanase, Glu78Asp, and IAA-Glu78Cys the calculated slope (β_{1g}) and the correlation coefficient (ρ) are $\beta_{1g} = -0.7$, $\rho = 0.97$; $\beta_{1g} = -0.6$, $\rho = 0.8$; and $\beta_{1g} = -0.8$, $\rho = 0.94$, respectively.

The pH Dependence of k_{cat}/K_m. Values of k_{cat}/K_m for the hydrolysis of ONPX_2 by native xylanase and IAA-Glu78Cys were determined as a function of pH as described in Experimental Procedures. Previous work had indicated that the IAA-Glu78Cys mutant is relatively unstable over long periods at 40 °C; thus, these studies were performed at 25 °C, a temperature at which the modified mutant is stable over the pH range 3.5−7.5. Analysis of the resulting plot of k_{cat}/K_m versus pH, illustrated in Figure 7, yielded the following pK_a values for native xylanase (pK_{a1} = 4.6 ± 0.04, pK_{a2} = 6.8 ± 0.03) and IAA-Glu78Cys (pK_{a1} = 3.3 ± 0.08, pK_{a2} = 6.5 ± 0.07).

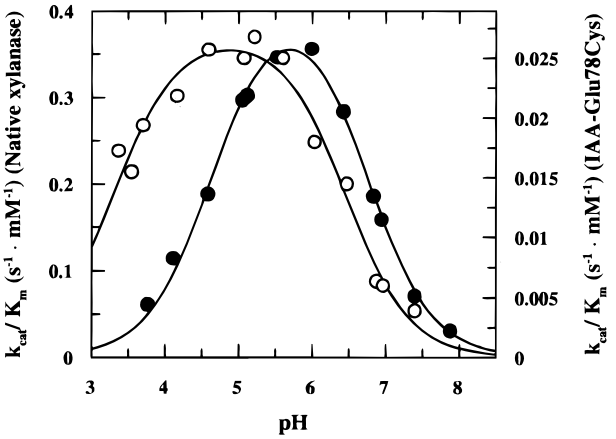

FIGURE 7: pH dependence of k_{cat}/K_m for native xylanase (●) and IAA-Glu78Cys (○) prepared under denaturing conditions. The lines shown represent fits to data for an enzyme with two ionizing groups as described in Results.

DISCUSSION

Replacement of Glu78, the active site nucleophile, with a cysteine had a dramatic effect on enzymatic activity, the apparent k_{cat} value for the Glu78Cys mutant being decreased at least 7×10^6-fold relative to native xylanase (Table 1). However, even this activity appears to be due to a contaminant as revealed by the inactivation behavior with 2F-$DNPX_2$; thus it appears that the Cys mutant is essentially devoid of activity. This inactivity is not the result of a disrupted secondary structure, as indicated by CD analysis, but is most likely due to the inability of Cys78 to act as the active site nucleophile/leaving group. The possibility that the enzyme was forming a stable thioglycoside intermediate, via initial attack of the thiol, was investigated by incubating the mutant with 2,5-$DNPX_2$ and monitoring for a burst of release of 2,5-dinitrophenolate. No such burst was observed and neither was a mass increase of the enzyme observed by ESMS.

While thiol groups are typically good nucleophiles, it is likely that the cysteine side chain is not close enough to attack the substrate's anomeric carbon. To probe this, the probable active site environment of the Glu78Cys mutant was examined by molecular modeling using the published X-ray crystal structure (Campbell et al., 1993). Replacement of Glu78 by a cysteine revealed that the thiol group is ~2 Å farther removed from the anomeric carbon of the scissile bond than the oxygens of the carboxylate group of Glu78 (5.3 and 3.4 Å, respectively). Indeed, the thiol group appears to be only poorly accessible to anionic labeling reagents since it proved impossible to selectively modify this cysteine with iodoacetate under nondenaturing conditions, even though this is the only thiol in the protein. The best IAA labeling conditions discovered yielded a population of enzyme species of which only 7% was active. While treatment with mild denaturants did speed up the reaction rate, it did not increase the overall activity regain.

The IAA labeling of Glu78Cys under denaturing conditions (7.1 M urea, ~10 times excess IAA, pH 7) proved to be a much better method to selectively and completely carboxymethylate Cys78. ESMS analysis and thiol titrations indicated that >90% of Cys78 had been selectively carboxymethylated, while the active site titration estimated greater than 90% active enzyme. Assays with a range of substrates (Table 1) revealed that the IAA-modified Glu78Cys mutant prepared in this way is highly active with a range of aryl xylobioside substrates. Values of k_{cat} are reduced only some 3−10-fold relative to native xylanase, and binding (as indicated by K_m values) is only slightly perturbed despite the increased bulk of the enzymic nucleophile. It was therefore necessary to ensure that the modified enzyme was still operating through a retaining (double-displacement) mechanism involving a glycosyl−enzyme intermediate. This is particularly important in light of the recent demonstration that glycosidases can change mechanism if appropriately mutated (Kuroki et al., 1995; Wang et al., 1994). We first followed the stereochemical course of the reaction by ^1H NMR spectroscopy, and the enzyme clearly yielded a product of retained stereochemistry. We then used the mechanism-based inhibitor 2F-$DNPX_2$ and the associated mass increase of the enzyme to clearly implicate a covalent glycosyl−enzyme intermediate, thus a retaining mechanism. Further evidence that the intermediate formed involved the carboxymethylated Cys78 was obtained from the mass spectrometric identification of the glycosylated peptide as one including the modified Cys78. The catalytic competence of the intermediate trapped in this way was demonstrated by the reactivation of the purified trapped intermediate upon incubation, either by hydrolysis or, in the presence of xylobiose, by transglycosylation. These results provide strong evidence that the carboxymethylated Glu78Cys mutant is catalytically active and functions via a double-displacement mechanism in which the carboxymethylated cysteine acts as the catalytic nucleophile.

Comparison of the dependence upon pH of k_{cat}/K_m for hydrolysis of $ONPX_2$ by wild-type and IAA-Glu78Cys reveals very little difference in pK_{a2}, but a significant decrease in pK_{a1} as a consequence of replacement of Glu78 by the carboxymethylated cysteine. These pK_a values reflect ionizations in the free enzyme, with pK_{a1} most likely reflecting the ionization of the catalytic nucleophile and pK_{a2} reflecting the ionization of the acid/base catalyst. The absence of any significant effect on pK_{a2} is certainly in line with this suggestion and indicates that no significant structural changes occur at the active site which affect the environment of Glu172. The depression in pK_{a1} is most likely a consequence of an inductive effect from the thioether linkage. Indeed, a comparison of the pK_a values of the analogous carboxylic acids $CH_3CH_2CO_2H$ (pK_a = 4.88) and $CH_3SCH_2CO_2H$ (pK_a = 3.72) reveals a pK_a depression of approximately 1 pH unit (Brown et al., 1955).

Native xylanase catalyzed the hydrolysis of a range of aryl xylobiosides, with k_{cat}/K_m values (which reflect the first irreversible step, most likely glycosylation) increasing in step with the aglycon leaving group ability. Indeed, a reasonable linear correlation is observed between log k_{cat}/K_m and the aglycone pK_a. The slope of this Brønsted plot ($\beta_{1g} = -0.7$) indicates very substantial glycosidic bond cleavage at the glycosylation transition state with very little proton donation. Interestingly a very similar relationship is observed for IAA-Glu78Cys, with there being essentially no difference in the slopes within the error of their determination. A very similar trend is observed for the Glu78Asp mutant, even though data for this mutant are limited. This implies that even though there are substantial effects on rate due to changes in the nucleophile position, there is very little effect on the reaction mechanism, at least with respect to charge development on

the aglycon oxygen. The linear relationships in these plots demonstrate that the step being monitored is indeed the glycosylation step in all cases. Interestingly, the rate difference (k_{cat}/K_m) observed for 2,5-DNPX_2 between wild-type and IAA-Glu78Cys (16-fold) is very similar to the difference in the inactivation rates with 2F-DNPX_2. This is reasonable as both reflect rates of formation of the glycosyl−enzyme intermediate.

Comparison of the kinetic parameters for the IAA-Glu78Cys mutant with those for wild-type and the Glu78Asp mutant allows some insight into the effects of changing the position of the catalytic nucleophile. The effects of shortening the nucleophile on rate are significant with the k_{cat}/K_m values, reflecting the glycosylation step, being reduced some 1600−5000-fold relative to wild-type enzyme. This rate reduction is consistent with that seen in other glycosidases modified in this same manner and studied to this extent (Withers et al., 1992; Yuan et al., 1994). Thus, a severe price is paid for increasing the distance between the carboxylate and the developing positive charge at the transition state. This is most likely accommodated, at least in part, by a slight dislocation of the sugar within its binding site. What is perhaps surprising is how small the effects of lengthening the nucleophile are, with k_{cat}/K_m values being reduced only 16−100-fold relative to wild type and k_{cat} values much less. This presumably indicates that there is sufficient room at the active site for the side chain to fold down and adopt a position in which the carboxylate can function effectively as a nucleophile. Indeed, molecular modeling studies in which a carboxymethyl group was built onto Cys78 confirmed that such space is available. A much smaller price is therefore paid, the rate decreases reflecting the steric and entropic costs of folding up the lengthened side chain. These rate differences do not, however, appear to be reflected in the degree of bond cleavage or proton donation at the glycosylation transition state as demonstrated by the similar β_{1g} values. Thus, the relatively fixed environment of the active site dictates a very similar transition state structure in each case; however, that transition state structure is less frequently attained when the carboxylate is imperfectly aligned.

ACKNOWLEDGMENT

We thank Dave Burgoyne, Curtis Braun, and David Chow for the MS work, René Lemieux for technical assistance with the NMR study, and Lawrence McIntosh and Manish Joshi for helpful discussions and assistance with the molecular modeling. Thanks are also extended to Dr. Lothar Ziser for providing the xylobioside substrates and inactivator.

REFERENCES

Amano, T., Tozawa, K., Yoshida, M., & Murakami, H. (1994) *FEBS Lett. 348*, 93−98.
Bray, M. R., & Clarke, A. J. (1990) *Biochem. J. 270*, 91−96.
Brown, H. C., McDaniel, D. H., & Häfliger, O. (1955) in *Determination of Organic Structures by Physical Methods* (Braude, E. A., & Nachod, F. C., Eds.) pp 567−662, Academic Press, New York.
Campbell, R., Rose, D., Wakarchuk, W., To, R., Sung, W., & Yaguchi, M. (1993) in *Proceedings of the 2nd TRICEL symposium on Trichoderma reesei cellulases and other hydrolases* (Suominen, P., & Reinikainen, T., Eds.) pp 63−72, Foundation for Biotechnical and Industrial Fermentation Research, Helsinki, Finland.
Davies, G., & Henrissat, B. (1995) *Structure 3*, 853−859.
Dhalla, A. M., Li, B., Alibhai, M. F., Yost, K. J., Hemmingsen, J. M., Atkins, W. M., Schineller, J., & Villafranca, J. J. (1994) *Protein Sci. 3*, 476−481.
Ellman, E. L. (1959) *Arch. Biochem. Biophys. 82*, 70−77.
Gebler, J., Gilkes, N. R., Claeyssens, M., Wilson, D. B., Beguin, P., Wakarchuk, W., Kilburn, D. G., Miller, R. C., Jr., Warren, R. A. J., & Withers, S. G. (1992) *J. Biol. Chem. 267*, 12559−12561.
Gilkes, N. R., Henrissat, B., Kilburn, D. G., Miller, R. C., Jr., & Warren, R. A. J. (1991) *Microbiol. Rev. 55*, 303−315.
Gloss, L. M., & Kirsch, J. F. (1995) *Biochemistry 34*, 3990−3998.
Henrissat, B., & Barrioch, H. (1993) *Biochem. J. 293*, 781−788.
Hess, D., Covey, T. C., Winz, R., Brownsey, R., & Aebersold, R. (1993) *Protein Sci. 2*, 1342−1351.
Katsube, Y., Hata, Y., Yamaguchi, H., Moriyama, H., Shinmyo, A., & Okada, H. (1990) in *Protein Engineering: Protein Design in Basic Research, Medicine and Industry* (Ikehara, M., Ed.) pp 91−96, Japan Scientific Societies Press, Tokyo.
Ko, E. P., Akatsuka, H., Moriyama, H., Shinmyo, A., Hata, Y., Katsube, Y., Urabe, I., & Okada, H. (1992) *Biochem. J. 288*, 117−121.
Koshland, D. E. (1953) *Biol. Rev. 28*, 416−436.
Kuroki, R., Weaver, L. H., & Matthews, B. W. (1995) *Nature Struct. Biol. 2*, 1007−1011.
Leatherbarrow, R. J. (1990) GraFit version 3.0, Erithacus Software Ltd., Staines, U.K.
Lukac, M., & Collier, R. J. (1988) *J. Biol. Chem. 263*, 6146−6149.
Matsushima, Y., Kim, D., Yoshimura, T., Kuramitsu, S., Kagamiyama, H., Esaki, N., & Soda, K. (1994) *J. Biochem. (Tokyo)-115*, 108−112.
McCarter, J., & Withers, S. G. (1994) *Curr. Opin. Struct. Biol. 4*, 885−892.
Miao, S., Ziser, L., Aebersold, R., & Withers, S. G. (1994) *Biochemistry 33*, 7027−7032.
Oku, T., Roy, C., Watson, D. C., Wakarchuk, W., Campbell, R., Yaguchi, M., Jurasek, L., & Paice, M. G. (1993) *FEBS Lett. 334*, 296−300.
Planas, A., & Kirsch, J. F. (1991) *Biochemistry 30*, 8268−8276.
Sinnott, M. L. (1990) *Chem. Rev. 90*, 1171−1202.
Smith, H. B., & Hartman, F. C. (1988) *J. Biol. Chem. 263*, 4921−4925.
Sung, W. L., Luk, C. K., Zahab, D. M., & Wakarchuk, W. (1993) *Protein Express. Purif. 4*, 200−206.
Wakarchuk, W. W., Campbell, R. L., Sung, W. L., Davoodi, J., & Yaguchi, M. (1994) *Protein Sci. 3*, 467−475.
Wang, Q., Graham, R. W., Trimbur, D., Warren, R. A. J., & Withers, S. G. (1994) *J. Am. Chem. Soc. 116*, 11594−11595.
Withers, S. G., Rupitz, K., Trimbur, D., & Warren, R. A. J. (1992) *Biochemistry 31*, 9979−9985.
White, A., Withers, S. G., Gilkes, N. R., & Rose, D. R. (1994) *Biochemistry 33*, 12546−12552.
Yuan, J., Martinez-Bilbao, M., & Huber, R. E. (1994) *Biochem. J. 299*, 527−531.
Ziser, L., & Withers, S. G. (1994) *Carbohydr. Res. 265*, 9−17.
Ziser, L., Setyawati, I., & Withers, S. G. (1995) *Carbohydr. Res. 274*, 137−153.

BI960586V